Geomechanics and Engineering, *Vol. 11, No. 4 (2016) 571-585*
DOI: http://dx.doi.org/10.12989/gae.2016.11.4.571

Assessment of the crest cracks of the Pubugou rockfill dam based on parameters back analysis

Wei Zhou [1], Shao-Lin Li [1,2], Gang Ma [*1],
Xiao-Lin Chang [1], Yong-Gang Cheng [1] and Xing Ma [1]

[1] *State Key Laboratory of Water Resources and Hydropower Engineering Science, Wuhan University, Wuhan, 430072, China*
[2] *Changjiang Institute of Survey, Planning, Design and Research, Wuhan 430010, China*

(*Received May 20, 2015, Revised October 22, 2015, Accepted June 06, 2016*)

Abstract. The crest of the Pubugou central core rockfill dam (CCRD) cracked in the first and second impounding periods. To evaluate the safety of the Pubugou CCRD, an inversion analysis of the constitutive model parameters for rockfill materials is performed based on the in situ deformation monitoring data. The aim of this work is to truly reflect the deformation state of the Pubugou CCRD and determine the causes of the dam crest cracks. A novel real-coded genetic algorithm based upon the differences in gene fragments (DGFX) is proposed. It is used in combination with the radial based function neural network (RBFNN) to perform the parameters back analysis. The simulated settlements show good agreements with the monitoring data, illustrating that the back analysis is reasonable and accurate. Furthermore, the deformation gradient of the dam crest has been analysed. The dam crest has a great possibility of cracking due to the uncoordinated deformation, which agrees well with the field investigation. The deformation gradient decreases to the value lower than the critical one and reaches a stable state after the second full reservoir.

Keywords: high central core rockfill dam; dam crest cracks; monitoring data analysis; parameters back analysis; uncoordinated deformation

1. Introduction

Rockfill dams are one of the most preferred dam types in hydraulic engineering because of their simple construction sequence, short construction period and good seismic performance. They are currently constructed with great frequency throughout the world. Over the past two decades, many rockfill dams whose height is 150 m to 240 m have been built in China. At present, a growing number of rockfill dams are being built in western China. The height of most dams is above 200 m, and some are even higher than 300 m. Due to the great height and large storage capacity of the dams, the safety of these high dams is a major concern that attracts the attention of engineers and scientific researchers.

The dam crest of the Pubugou CCRD cracked in the first and second impounding periods. In CCRDs, the central core rockfill zone plays an important role as a watertight core. Any cracks in

*Corresponding author, Lecturer, E-mail: magang630@whu.edu.cn

http://www.techno-press.org/?journal=gae&subpage=7 ISSN: 2005-307X (Print), 2092-6219 (Online)

the central core rockfill zone will impair the integrity of the seepage control system and weaken the structure or even threaten the safety of the dam. So it is significant to evaluate whether the cracks will develop into the central core rockfill zone or become stable after being repaired.

Time-dependent and wetting deformations are two most important characteristics of high rockfill dams and they play a key role in the dam safety. The finite element method (FEM) has been used to predict the deformation and stress of CCRD based on the mechanical parameters obtained from laboratory tests. However, due to the scaling effect, random sampling, and sample disturbance, the in situ mechanical properties of rockfills may differ from those obtained from laboratory tests (Gikas and Sakellariou 2008, Yu *et al*. 2007, Hua and Zhou 2010). Therefore, to gain a better understanding of the dam deformation characteristics, an inversion analysis of the parameters for rockfill materials has been performed based on the in situ deformation monitoring data (Szostak-Chrzanowski and Chrzanowski 2005, Szostak-Chrzanowski *et al*. 2006, Yu *et al*. 2007, Zhou *et al*. 2011). Since the Pubugou dam is the second largest CCRD ever built in China, it is necessary to find out the causes of the dam crest cracks and evaluate the safety of the dam based upon the identified parameters.

This paper analysed the deformation monitoring data of the Pubugou CCRD, whose crest cracked in the first and second impounding periods. A novel real-coded genetic algorithm based upon the differences of gene fragments (DGFX) was proposed and it was used in combination with the RBFNN to perform the parameters back analysis. On the basis of the identified parameters, the time-dependent deformation of the dam was predicted. Moreover, the deformation gradient were calculated to find out the causes of the dam crest cracks, and the safety of the dam was evaluated.

2. Brief description of the Pubugou CCRD

The Pubugou dam, shown in Fig. 1, was built on the Dadu River and situated between Hanyuan and Ganluo, Sichuan Province, China. The height of Pubugou dam is 178 m, and the length of the dam crest is 540.5 m, other details are given in (Table 1). Fig. 2 shows the plane layout of the Pubugou Dam. The dam body mainly consists of two parts: compacted rockfills and earth core. The impervious core with slopes of 1:0.25 was placed at the central of the dam. The finite element mesh of the Pubugou dam is shown in Fig. 3.

Table 1 General characteristics of the Pubugou CCRD

Maximum height	178 m
Crest elevation	854 m
Crest length	540.5 m
Crest width	14 m
Dam volume	22,370,000 m^3
Operational water level	850 m
Reservoir volume	5,337,000,000 m^3
Number of generators	6
Installed capacity	3600 MW
Annual energy generation	14,790,000,000 kw•h

Fig. 1 A general view of the Pubugou CCRD

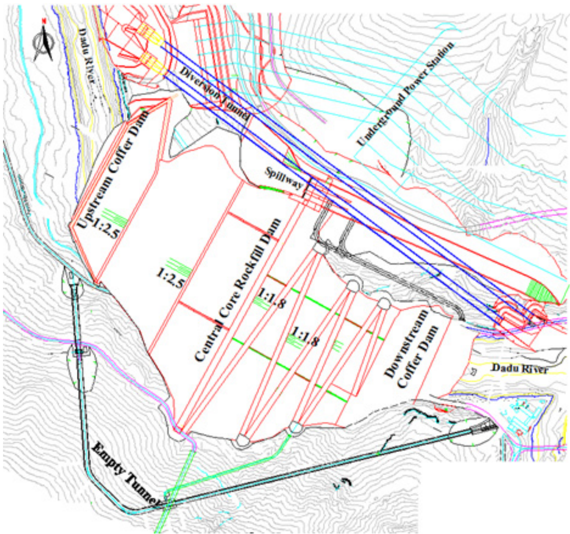

Fig. 2 The plane layout of the Pubugou CCRD

Fig. 3 The finite element model of the Pubugou Dam

The construction of the dam began in 2006 and completed in 2009. The reservoir began impounding in September 2009 and was full by October 2010. A crack was found in the crest with a width of 3 cm when the reservoir level was approximately 850 m. In October 2011, the water level reached 850 m again. In the second impounding period, another crack appeared at the crest with a width of 1 cm and a depth of 1.5 m.

3. Deformation monitoring analysis

Due to the paramount significance of the project, an improved and detailed deformation monitoring system has been adopted in the Pubugou CCRD. The vertical deformation inside the dam body is measured by a series of hydraulic overflow settlement gauges, which are distributed in four sections: 0+128, 0+240, 0+310, and 0+431. Section 0+240 is the largest cross section of the Pubugou CCRD. More specifically, eight monitoring lines have been placed in the four sections, three lines each in sections 0+240 and 0+310 (at elevations of 731, 758 and 808 m, respectively) and one each in sections 0+128 and 0+431 (at elevations of 808 m). For central core rockfill dam, most of the upstream rockfill are submerged under water. Therefore the hydraulic overflow settlement gauges are just placed at the downstream. The layout of the in situ monitoring gauges in section 0+240 is shown in Fig. 4.

The settlement monitoring data is from March 2008 to December 2011, nearly 4 years, covering the construction period and 2 years of operation. The settlements of all monitoring points

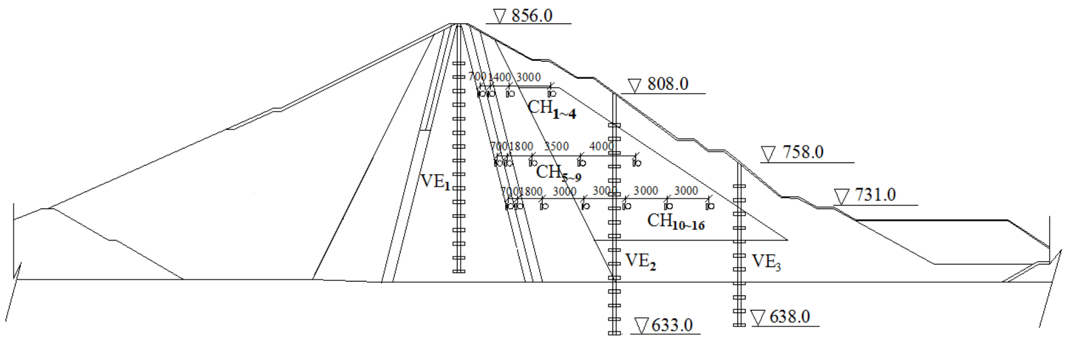

Fig. 4 Layout of the monitoring system in section 0+240 of the Pubugou CCRD

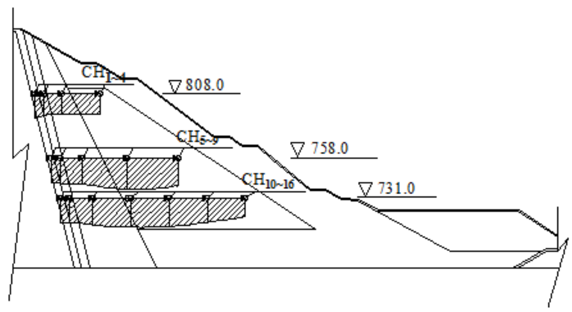

Fig. 5 Internal settlements observed in section 0+240 in December 2011

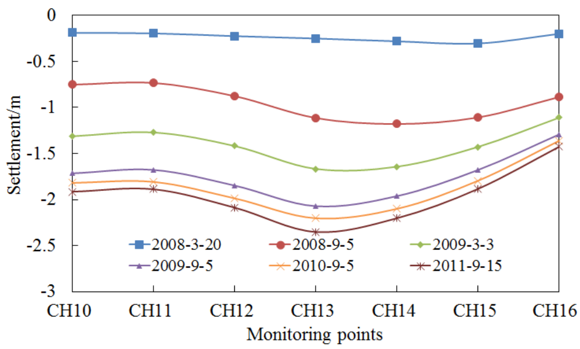

Fig. 6 Settlements of the monitoring points (CH10-CH16) from March 2008 to September 2011

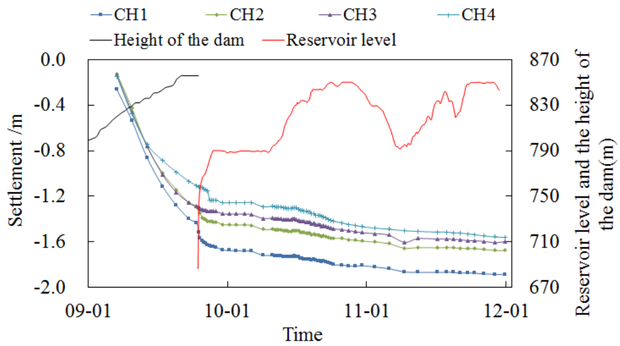

(a) At the elevation of 808 m

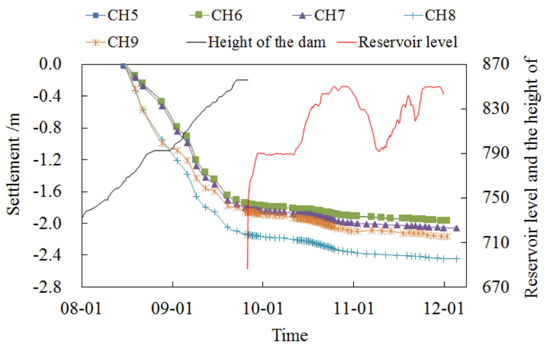

(b) At the elevation of 758 m

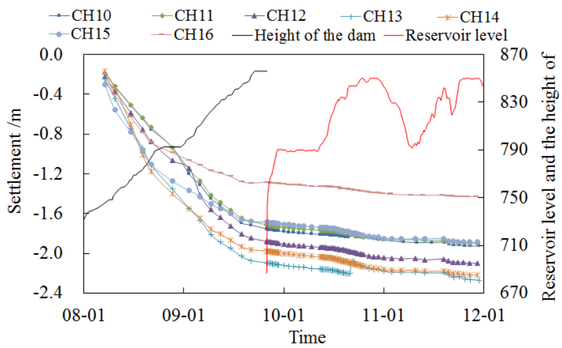

(c) At the elevation of 731 m

Fig. 7 Settlements recorded in section 0+212

in section 0+240 are analysed to reveal the vertical deformation inside the dam body. The development of settlement is divided into three stages, i.e., the construction (before November 2009), first impounding period (November 2009 to November 2010), and operation stages (November 2010 to December 2011).

Fig. 5 shows the distribution of the settlement in section 0+240 m in 2011. Fig. 6 illustrates the settlements of the monitoring points at the elevation of 731 m at different times. Two conclusions can be drawn from the plots: first, the settlement in the central part of the downstream material zone is larger than that in the central core zone and the downstream shell; second, most of the settlement occurred in the construction and the first impounding period.

The evolution of the settlement observed by hydraulic overflow settlement gauges in section 0+240 is shown in Fig. 7. The largest settlement is 2.444 m (approximately 1.37% of the dam height), which appears at an elevation of 758 m in the downstream section. The deformation developed rapidly during the construction and the first impounding period and decreased progressively over time. More than 80% of the settlement developed before November 2009, and the remaining 20% developed during first reservoir filling and operation period, which also suggests that the dam tended to be stable. Moreover, on average, the development of settlement exhibits similar trends, suggesting that the monitoring system works well and can reflect the deformation characteristics of the Pubugou CCRD.

4. Parameters back analysis using RBFNN and modified genetic algorithm

4.1 Constitutive model

The Duncan & Chang E-B model (Duncan *et al*. 1980) is one of the most commonly used nonlinear elastic constitutive models. It is used to describe the nonlinear elastic behaviour of the rockfills in this paper. There are eight parameters in the Duncan & Chang E-B model, i.e., c, φ, $\Delta\varphi$, R_f, K, n, K_b, and m, which can be determined by conventional triaxial tests of rockfill materials.

The time dependent deformation is another important property of rockfill materials. In this study, the Merchant creep model with seven parameters (Li *et al*. 2004) is used.

The creep strain ε_t is expressed as follows

$$\varepsilon_{\mathrm{t}} = \varepsilon_{\mathrm{f}}(1 - e^{-\alpha t}) \tag{1}$$

where ε_f is the limit of the creep strain, and α is a coefficient related to the creep strain rate. The limit of creep strain ε_f can be divided into the limit of volume creep strain ε_{vf} and shear creep strain ε_{sf}. The limit of volume creep strain ε_{vf}, determined by the minor principal stresses σ_3 and the deviatoric stress is given by the following relationship

$$\varepsilon_{\mathrm{vf}} = b\left(\frac{\sigma_3}{p_{\mathrm{a}}}\right)^{M_{\mathrm{c}}} + \beta\left(\frac{q}{p_{\mathrm{a}}}\right)^{N_{\mathrm{c}}} \tag{2}$$

where σ_3 is the confining pressure, q is the deviatoric stress, and b, β, M_c, and N_c are the creep parameters.

The limit of shear creep strain ε_{sf} is associated with the stress level S_L, as given below

$$\varepsilon_{\mathrm{sf}} = d\left(\frac{S_{\mathrm{L}}}{1 - S_{\mathrm{L}}}\right)^{l_{\mathrm{c}}} \tag{3}$$

where S_L is the stress level, and d and l_c are the creep parameters.

There are seven parameters in the creep model, α controls the creep strain rate, b, β, M_c, and N_c

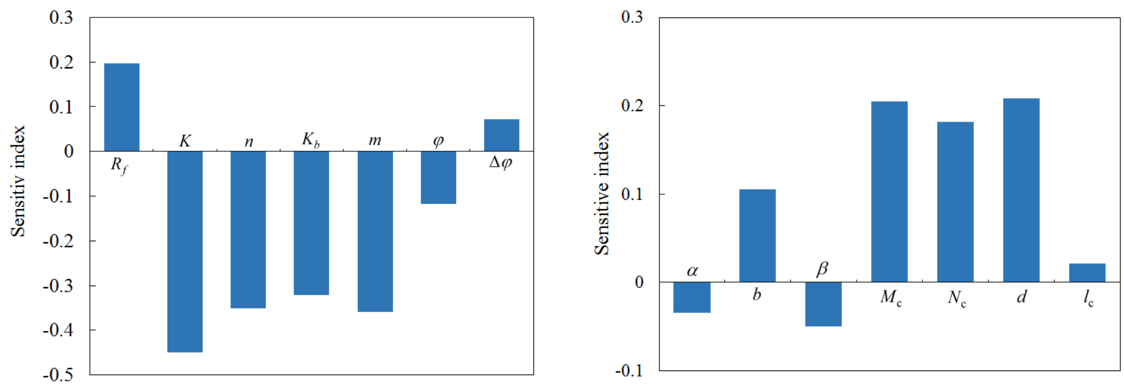

(a) Duncan & Chang E-B model (b) Merchant creep model

Fig. 8 The parametric sensitivity analysis

are defined for the limit of creep strain and d and l_c are defined for volume creep. All of the parameters can be determiend using a set of creep triaxial tests.

4.2 Parameters sensitivity analysis

As described above, in the constitutive model of rockfill materials, fourteen parameters need to be identified. In addition, when considering dam material zoning, the number of parameters to be identified will be very large. Therefore, it is necessary to perform a parameters sensitivity analysis for selecting the most sensitive parameters.

Morris' method (Morris 1991, Tomlin 2006) is currently the most used method. By perturbing each parameter independently, Morris' method adopts the sensitive indicators S to reflect the sensitivity of the parameters

$$S = \frac{1}{q-1}\sum_{i=1}^{q-1}\frac{\left(Y_{\mathrm{i+1}} - Y_{\mathrm{i}}\right)/Y_0}{\left(P_{\mathrm{i+1}} - P_{\mathrm{i}}\right)/P_0} \tag{4}$$

where S is the parameter sensitivity index, Y_0 is the calculated deformation using the initial parameters, Y_i is the calculated deformation of the i^{th} time, P_i is the material parameters of the ith calculation, P_0 is the initial parameters and q is the total number of calculations.

As shown in Fig. 8, the most sensitive parameters of the E-B model and creep model are K, n, K_b, m, M_c, N_c and d. Therefore, we only perform back analysis on these parameters mentioned above. In laboratory test, the creep deformation often stabilizes in a few hours, whereas the deformation of a rockfill dam continues for more than several years. Thus, the parameter α is chosen to be identified as well.

4.3 A modified genetic algorithm

The parameters back analysis can be categorized as an optimization problem in mathematics. A variety of population-based probabilistic techniques have been proposed in the literature to solve the optimization problems, including the genetic algorithm (GA) (Holland 1975, John 1992), simulated annealing (SA) (Dowsland and Thompson 2012, Van Laarhoven and Aarts 1987), and particle swarm optimization (PSO) (Eberhart and Kennedy 1995, Ma *et al*. 2012). Among these algorithms, the GA has proven to be a powerful tool in solving optimization problems.

The crossover operator is a determinant key in genetic algorithm. It controls the diversity of the population and the disproportionation between exploitation and exploration, and influences the global convergence of the algorithm. In simple genetic algorithm, the crossover points and gene fragments are randomly selected. It is difficult to generate new individuals when the selected gene fragments are the same or highly similar.

Inspired by genetic engineering and the cloning of superior genes, a novel genetic crossover operator based on the differences in gene fragments (DGFX) is proposed to improve the genetic algorithm. The fragments' crossing probabilities are evaluated based on the differences of themselves, and the selected gene fragments are then exchanged based on the crossing probability. This process reduces inbreeding operation and increases the efficiency of the crossover.

The gene fragment is a continuous set of genes with a random length, and the crossover point is the first gene of the fragment. The differences in gene fragment $D(j)$ is defined as follows

$$D(j) = \frac{1}{l}\sum_{i=j}^{(j+l-1)} abs(x_i^{(1)} - x_i^{(2)}), \qquad j = (1, 2, \cdots, n-l+1) \tag{5}$$

where l is the length of the gene fragment, $x_i^{(1)}$ and $x_i^{(2)}$ are the i^{th} genes of the chromosome $x^{(1)} = (x_1^{(1)}, x_2^{(1)}, \cdots, x_n^{(1)})$, and $x^{(2)} = (x_1^{(2)}, x_2^{(2)}, \cdots, x_n^{(2)})$, and n is the length of the chromosome. The gene fragment j is selected to intersect according to the probability

$$P(j) = \frac{D(j)}{\sum_{i=1}^{(n-l+1)} D(i)}, \qquad j = (1, 2, \cdots, n-l+1) \tag{6}$$

where $D(i)$ and $D(j)$ are the differences in gene fragments i and j, respectively.

As shown in Fig. 9, the gene fragment difference has been calculated. The differences in the two chromosomes are 9 and 21, respectively. The first gene fragment (I) does not help much to produce better generations because the fragments are similar to each other. Due to the significant gene fragment differences, the second gene fragment has much higher potential to produce new generations significantly different from their parents. The greater the differences in the gene fragments are, the more likely that new generations would be generated, which can give the genetic algorithm a drastic acceleration for convergence. Upon this theory, an innovative crossover based on the differences in gene fragments is proposed, and the differences are calculated by Eq. (5). According to Eq. (6), the gene fragments are selected to intersect.

In the DGFX crossover operator, the convergence is significantly influenced by the length of gene fragment. The length of gene fragments is defined as follows

$$l = u_1 l_{\text{chrom}} I \tag{7}$$

where u_1 is a random number in the range of 0 to 1, l_{chrom} is the total length of the chromosome and I is the coefficient of the gene fragment. The coefficient I controls the length of the gene fragment, whereas u_1 increases the diversity of the crossover operation on the basis of the length coefficient. The concave strategy is used in this paper, and the length coefficient of the gene fragment can be

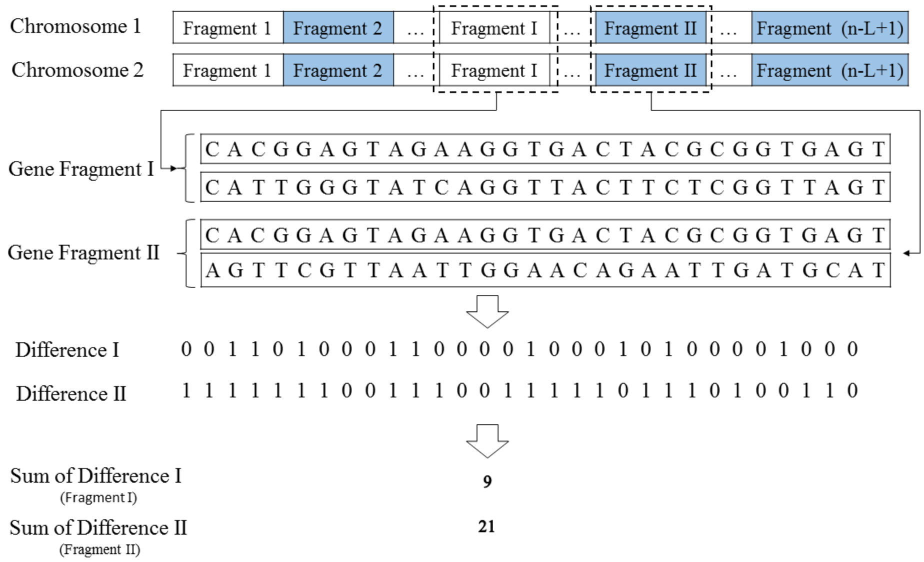

Fig. 9 The difference in gene fragments

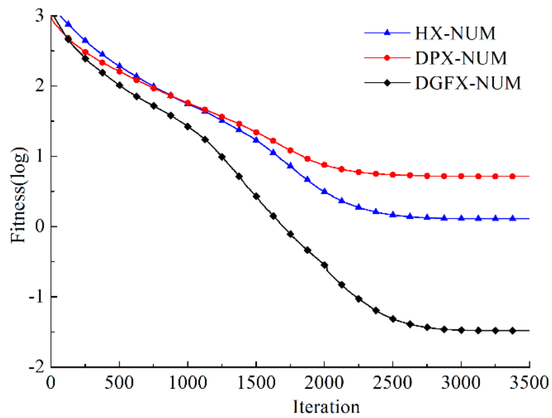

Fig. 10 Evolutions of the logarithmic average fitness for HX-NUM, DPX-NUM, and DGFX-NUM (All results are averaged over 30 runs)

obtained by the following equation

$$I = I_{\min} + (I_{\max} - I_{\min})\left(\frac{g}{G} - 1\right)^2 \tag{8}$$

where $I_{\min}$ and $I_{\max}$ are the minimum and maximum length coefficients of the gene fragment, respectively, g is the current iteration and G is the maximum iteration.

A modified GA named DGFX-NUM is developed by combining the DGFX operator and the non-uniform mutation (NUM) (Michalewicz 1996). To evaluate the performance of the proposed algorithm, two well-known crossover operators, DPX (Thakur 2014) and HX (Wright 1990), are selected for comparison using a benchmark function named Rastrigin (Ma *et al*. 2012). Similarly, the other GAs are named DPX-NUM and HX-NUM. As shown in Fig. 10, the proposed algorithm is more effective than the existing algorithms for nonlinear problems with large dimensionality, and it converges to satisfactory solutions more quickly.

4.4 Parameters back analysis method

The 2-norm of the difference between the calculated and observed displacements at the monitoring points can be taken as an objective function

$$f(\lambda_1,\lambda_2\ldots,\lambda_n)=\left[\frac{1}{n}\sum_{i=1}^{n}\left(\frac{u_{\mathrm{i}}-u_{\mathrm{i}}^{*}}{u_{\mathrm{i}}^{*}}\right)^2\right]^{0.5} \tag{9}$$

where λ_1, λ_2, ..., λ_n is a group of constitutive parameters need to be identified, u_i is the calculated deformation at the monitoring point i, u_i^* is the corresponding measured deformation and n is the number of monitoring points used in the back analysis.

To improve the computational efficiency, a radial basis function neural network (RBFNN) is constructed to map the relationship of constitutive parameters and the fitness of objective function. As shown in Fig. 11, the process of back analysis is expressed as follows:

(1) Firstly, a reasonable range is set according to field test and engineering analogy for each material parameter. Then some different values are selected uniformly within this range. The total computation time will be too long to accept if every possible combination of

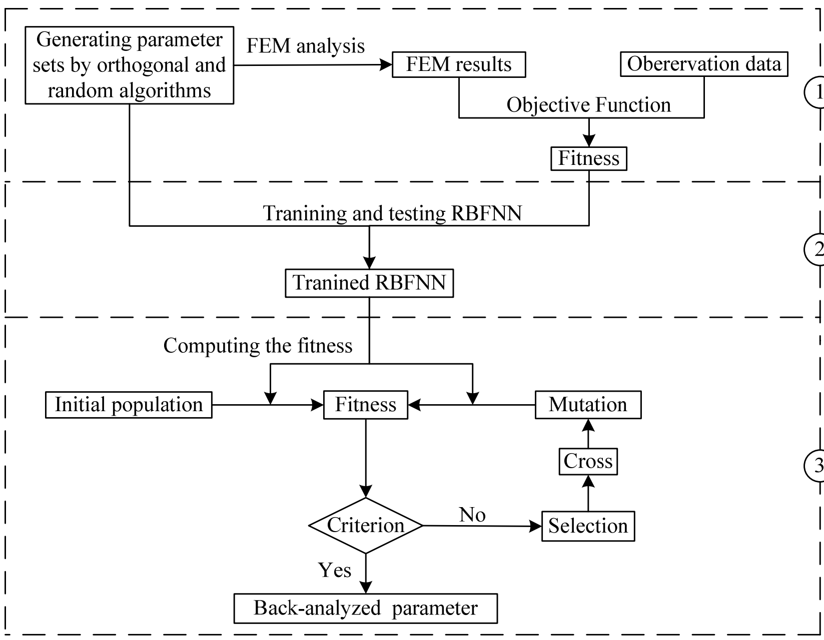

Fig. 11 The flow chart of parameters inversion based on the DGFX-NUM and RBFNN

material parameters was used to perform FEM calculation. To reduce the computational cost, the orthogonal arrays are used to generate some typical combinations of material parameters. Some other different combinations of material parameters are generated randomly to increase the robustness of samples. Then, instead of using each possible combination of material parameters, only these selected combinations are used to perform FEM calculation.

For all the combinations generated above, a non-linear FEM program that takes the static and creep properties of material into account is adopted to calculate the deformation of different monitoring points. Then fitness of the objective function are calculated using the simulated settlement and measured one.

(1) Different material parameter combinations and the calculated fitness of the objective points are used to train and test the RBFNN.

(2) Based on the monitoring data of settlement from all the observation points, the modified genetic algorithm (DGFX-NUM) is adopted to search optimal material parameters within their admissible ranges. The optimal parameters are a combination of material parameters that minimize the objective function. During the process of searching optimal material parameters, the trained RBFNN are used instead of the FEM to calculate the fitness of all the measurement points.

4.5 Parameters back analysis results

The identified parameters of the Duncan & Chang E-B model and creep model are presented in Table 3. The evolutions of settlement with time at two points in section 0+240 are shown in Fig. 12. The predicated settlement using the identified parameters and the measured settlement show

Table 2 Back-analysis results

Material zone	Creep model				E-B model			
	α (10^{-3})	M_c	N_c	d (10^{-3})	K	N	K_b	m
Central core rockfills	3.495	1.123	0.790	7.636	532	0.46	264	0.32
Secondary rockfills	1.218	0.952	0.544	7.271	807	0.40	462	0.37
Main rockfills	1.333	0.310	0.433	4.445	666	0.54	261	0.26

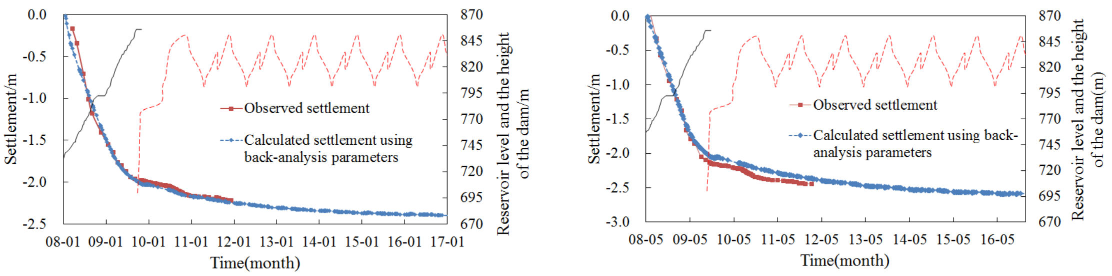

(a) At the elevation of 731 m (b) At the elevation of 758 m

Fig. 12 Evolutions of settlements with time in cross-section 0+240

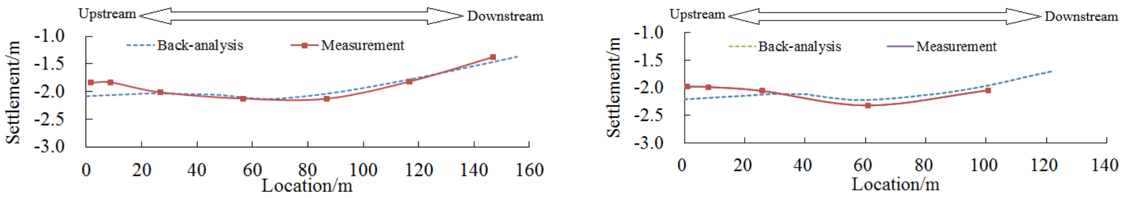

(a) At the elevation of 731 m (2011-12) (b) At the elevation of 758 m (2011-12)

Fig. 13 Comparisons between the settlement results of the measurement and back analysis

similar trends over time, and deviate little from each other. This indicates that the parameters back analysis is acceptable. Fig. 13 shows the comparisons of the predicated and measured settlements at two elevation of section 0+240 m in December 2012. The magnitude and distribution of the predicated settlements show good agreement with the measured ones.

5. Crest cracks analysis based on the identified parameters

To determine the causes of the cracks and the working conditions of the Pubugou dam, the settlement increment of the dam (shown in Figs. 14 and 15) is analysed based on the identified parameters. There is a significant settlement increment between the construction completion and the first full reservoir, especially the upstream side of the dam crest. The settlement increment of the upstream and the downstream is quite different. As shown in Fig. 15, the settlement increment between the first and the second full reservoir reduces, whereas the differences in the settlement increment between the upstream and downstream are still significant.

In addition, the degree of differential settlement can be reflected by the deformation gradient (Peng *et al*. 2013, Zhang *et al*. 2008). Therefore, the deformation gradient is used to evaluate the possibility of cracking. It can be calculated as follows

$$\gamma = \frac{S_a - S_b}{\left| X_a - X_b \right|} \times 100 \tag{10}$$

where γ is the deformation gradient of points a and b, X_a and X_b are the horizontal locations of them, and S_a and S_b are the cumulative settlements, respectively.

The crest points and deformation gradient are shown in Fig. 16. The legend “A-B” means the deformation gradient between point A and B, and it is same for “B-C”, “C-D” and “D-E”. The critical deformation gradient of fracture is usually determined by the centrifugal cracking modelling test of the rockfill materials. Although there are no test results for the Pubugou CCRD, the value is set as 0.1% according to the engineering analogy (Zhang *et al*. 2008). As shown in Fig. 16, the deformation gradient of the initial and the second reservoir filling periods are much greater than the critical deformation gradient. Therefore, the dam crest has a great possibility of cracking. It agrees well with the field investigation. The deformation gradient was smaller than the critical value in October 2012 and became stable soon afterwards.

It can be concluded from the above analysis that the crest cracks are caused by the uncoordinated deformation of the dam. According to the deformation gradient, the dam will not crack again after the second full reservoir.

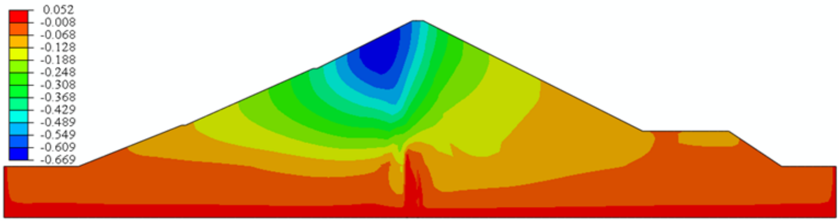

Fig. 14 Settlement increment between the time of completion and the first full reservoir (unit: m)

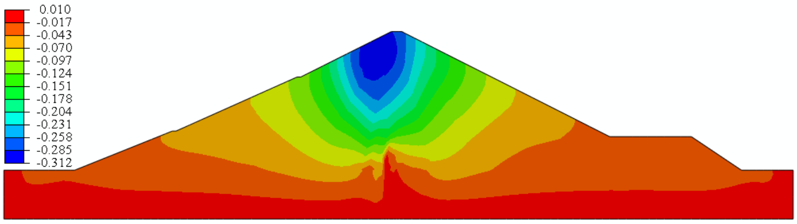

Fig. 15 Settlement increment between the first and the second full reservoir (unit: m)

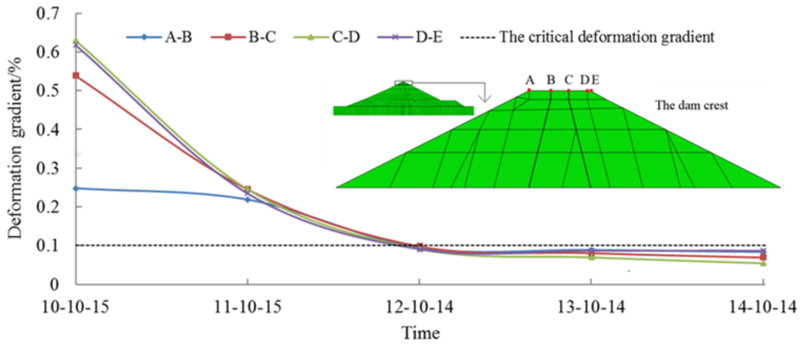

Fig. 16 Deformation gradient of the crest

6. Conclusions

The deformation characteristics of the Pubugou CCRD has been analyzed by the abundant monitoring data. A modified genetic algorithm has been proposed in this study and used in combination with the RBFNN to perform the parameters back analysis for rockfill materials. On the basis of the identified parameters, the deformation gradient of the dam crest has been analyzed. The primary findings drawn from this study are the following:

- According to the monitoring data analysis, the deformation of the Pubugou dam is in a reasonable range as a whole. The settlements developed during construction and the first impounding periods, then the settlement rate decreased with time and tended to be stabilized.
- The proposed genetic algorithm (DGFX-NUM) has better performance than the traditional ones. It reduces the inbreeding operation and increases the efficiency of the crossover, and has the advantage of a fast convergence rate and strong robustness.

- The simulated settlements show good agreements with the monitoring data, illustrating that the back analysis is acceptable.
- The results of the deformation gradient indicate that the crest cracks are caused by the uncoordinated deformation. In the first and second impounding periods, the deformation gradient was greater than the critical value, whereas in the next years, the deformation became stable and smaller than the critical value. The dam crest cracks will not propagate again.

Acknowledgments

This work was sponsored by the National Natural Science Foundation of China (No. 51322905 and No. 51379161) and China Postdoctoral Science Foundation (Grant No. 2015M572196).

References

Dowsland, K.A. and Thompson, J.M. (2012), Simulated Annealing, Springer, Berlin, Germany.

Duncan, J.M., Wong, K.S. and Mabry, P. (1980), “Strength, stress-strain and bulk modulus parameters for finite element analyses of stresses and movements in soil masses”, *Geotechnical Engineering*, University of California, CA, USA.

Eberhart, R.C. and Kennedy, J. (1995), “A new optimizer using particle swarm theory”, *Proceedings of the sixth International Symposium on Micro Machine and Human Science*, Nagoya, Japan, October.

Gikas, V. and Sakellariou, M. (2008), “Settlement analysis of the Mornos earth dam (Greece): Evidence from numerical modeling and geodetic monitoring”, *Eng. Struct.*, **30**(11), 3074-3081.

Holland, J.H. (1975), “Adaptation in natural and artificial systems”, University of Michigan, MI, USA

Hua, J.J., Zhou, W., Chang, X.L. and Zhou, C.B. (2010), “Study of scale effect on stress and deformation of rockfill”, *Chinese J. Rock Mech. Eng.*, **29**(2), 328-335.

John, H. (1992), *Holland*, *Adaptation in Natural and Artificial Systems*.

Li, G.Y., Mi, Z.K., Fu, H. and Fang, W.F. (2004), “Experimental studies on rheological behaviors for rockfills in concrete faced rockfill dam”, *Chinese J. Rock Soil Mech.*, **25**(11), 1712-1716.

Ma, G., Zhou, W. and Chang, X.L. (2012), “A novel particle swarm optimization algorithm based on particle migration”, *Appl. Math. Comput.*, **218**(11), 6620-6626.

Michalewicz, Z. (1996), *Genetic Algorithms + Data Structures = Evolution Programs*, Springer Science & Business Media.

Morris, M.D. (1991), “Factorial sampling plans for preliminary computational experiments”, *Technometrics*, **33**(2), 161-174.

Peng, Y., Zhang, Z.L., Zhang, B.Y. and Yuan, Y.R. (2013), “Deformation gradient finite element method for analyzing cracking in high earth-rack dam and its application”, *Chinese J. Rock Soil Mech.*, **34**(5), 1453-1458.

Szostak-Chrzanowski, A. and Massiéra, M. (2006), “Relation between monitoring and design aspects of large earth dams”, *Proceedings of the 3rd IAG Symposium on Geodesy for Geotechnical and Structural Engineering and 12-th FIG Symposium on Deformation Measurements*, Baden, Austria, May.

Szostak-Chrzanowski, A., Chrzanowski, A. and Massiéra, M. (2005), “Use of deformation monitoring results in solving geomechanical problems - Case studies”, *Eng. Geol.*, **79**(1-2), 3-12.

Thakur, M. (2014), “A new genetic algorithm for global optimization of multimodal continuous functions", *J. Computat. Sci.*, **5**(2), 298-311.

Tomlin, A.S. (2006), “The use of global uncertainty methods for the evaluation of combustion mechanisms”, *Reliab. Eng. Syst. Safe*, **91**(10-11), 1219-1231.

Van Laarhoven, P.J. and Aarts, E.H. (1987), *Simulated Annealing*, Springer, Netherlands.

Wright, A.H. (1990), "Genetic algorithms for real parameter optimization", *Found. Genetic Algorithms*, **1**, 205-218
Yu, Y., Zhang, B. and Yuan, H. (2007), "An intelligent displacement back-analysis method for earth-rockfill dams", *Comput. Geotech.*, **34**(6), 423-434.
Zhang, B.Y., Zhang, M.C. and Sun, X. (2008), "Centrifugal modeling of transverse cracking in earth core dams", *Chinese J. Rock Soil Mech.*, **29**(5), 1254-1258.
Zhou, W., Hua, J., Chang, X. and Zhou, C. (2011), "Settlement analysis of the Shuibuya concrete-face rockfill dam", *Comput. Geotech.*, **38**(2), 269-280.

GC